CONTENTS

JOURNAL OF RARE EARTHS
Vol. 38 No. 9 (September 2020)

CONTENTS

951 Facile synthesis of nanoceria by a molten hydroxide method and its photocatalytic properties

Xuewen Xia, Yuanpei Lan, Junqi Li**, Chaoyi Chen, Benjun Xu, Xian Luo, Xisong Mao*

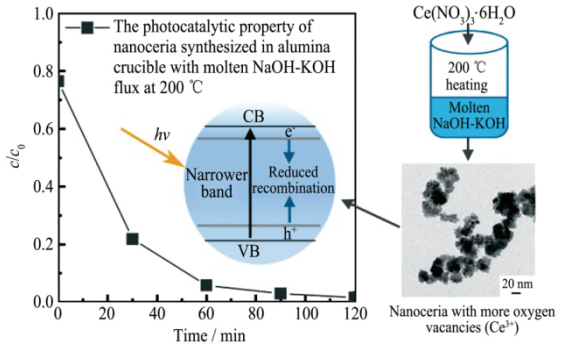

The nanoceria synthesized in alumina crucible with NaOH–KOH flux at 200 °C owns better photocatalytic property due to the narrower band gap and reduced recombination rate of electrons and holes

J. Rare Earths, (38) 2020: 951-960

MAGNETISM AND MAGNETIC MATERIALS

961 Systematic study of the dependence of magnetic and structural properties of $Nd_2Fe_{14}B$ powders on the average particle size

J.F. Durán Perdomo, G.A. Pérez Alcázar, H.D. Colorado, J.A. Tabares, L.E. Zamora, J.J.S. Garitaonandia*

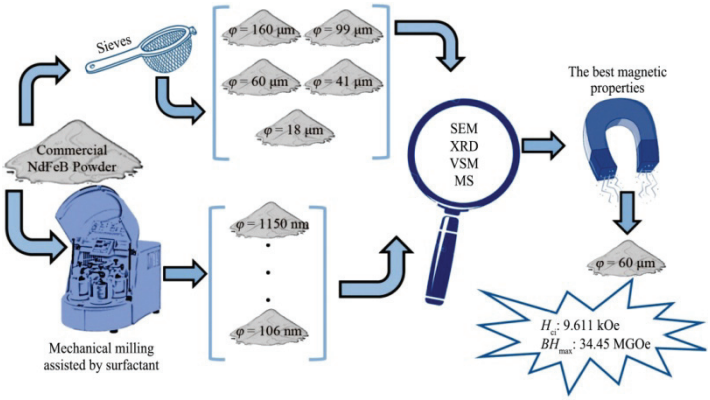

Preparation of the $Nd_2Fe_{14}B$ powders

J. Rare Earths, (38) 2020: 961-968

969 Investigation on the 773 K isothermal section of Ho-Ni-Si ternary phase diagram by X-ray powder diffraction and magnetic property of Ho_3NiSi_2 alloy

Xiang Chen, Jixin Gong, Jiaojiao Luo, Wenxuan Yang, Xian Qing*

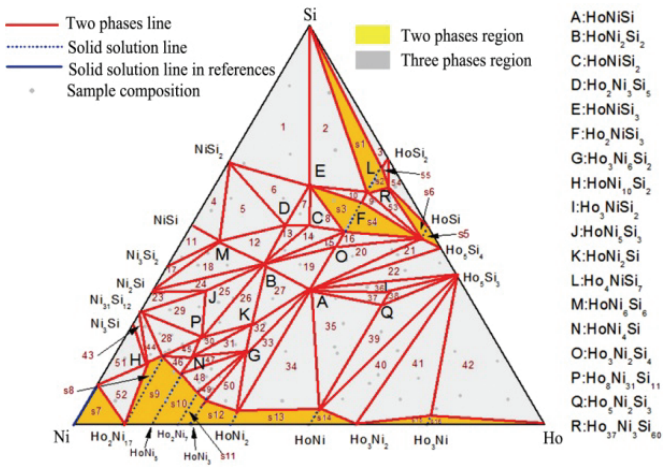

The Ho-Ni-Si ternary isothermal section phase diagram at 773 K

J. Rare Earths, (38) 2020: 969-975

ADVANCED RARE EARTH MATERIALS

976 Solution combustion synthesis and electrochemical properties of yttrium-doped $LiMnPO_4/C$ cathode materials for lithium ion batteries

Redouan El Khalfaouy, Servet Turan, Miguel A. Rodriguez, Kamil Burak Dermenci, Umut Savacı, Abdellah Addaou, Ali Laajeb, Ahmed Lahsini*

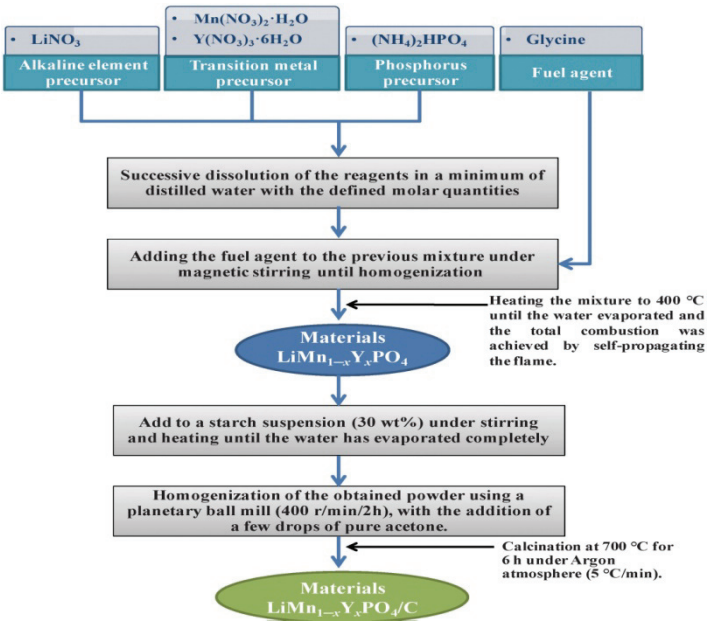

Solution combustion synthesis process of $LiMn_{1-x}Y_xPO_4/C$ cathode materials (x = 0, 0.01, 0.03, 0.05). Yttrium was successfully incorporated into the $LiMnPO_4$ host material structure, which can enhance its structural stability by improving ion transfer efficiency during charge/discharge process

J. Rare Earths, (38) 2020: 976-982

983 Enhanced hydrogen storage performance of Mg-Cu-Ni system catalyzed by CeO_2 additive

*Yi Yin, Bo Li, Zeming Yuan, Yan Qi, Yanghuan Zhang**

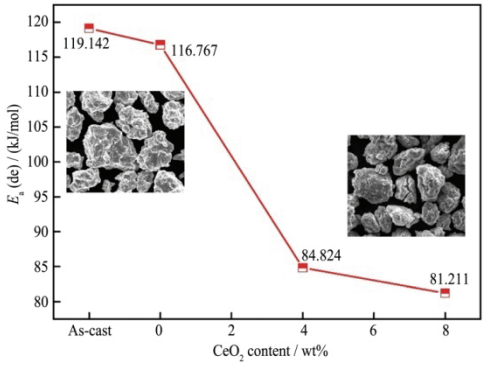

During hydriding and dehydriding, the cracks and defects formed on the CeO_2 catalyzed alloys particles enhance hydrogen storage kinetics

J. Rare Earths, (38) 2020: 983-993

CHEMISTRY AND HYDROMETALLURGY

994 Thermal decomposition mechanism of low-content-fluorite Bayan Obo rare earth concentrate roasted with sodium carbonate and its consequent separation study

Dan Zou, Ji Chen, Jiashi Hu, Kai Li, Deqian Li*

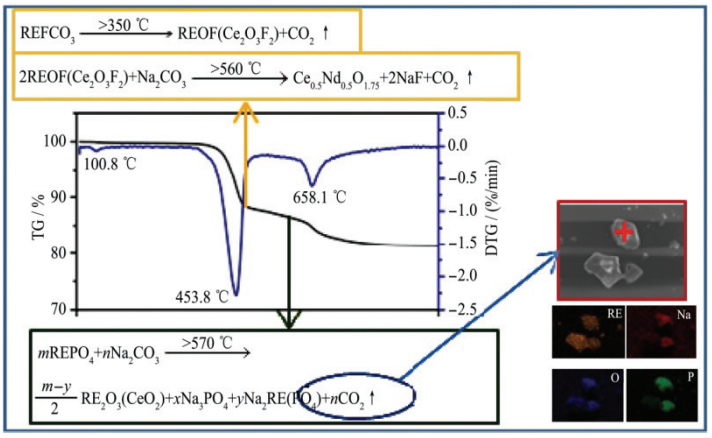

Thermal decomposition mechanism of Bayan Obo RE concentrate with low-content fluorite calcined with sodium carbonate and its technology study were investigated in this paper. During the calcination process, BORC, consisting of bastnaesite and monazite, is decomposed and transformed into $Ce_{0.5}Nd_{0.5}O_{1.75}$, NaF, Na_3PO_4, and a rare earth double phosphate phase $Na_3RE(PO_4)_2$

J. Rare Earths, (38) 2020: 994-1002

1003 Extraction of scandium from red mud by acid leaching with CaF_2 and solvent extraction with P507

Xiaobo Zhu, Wang Li, Baolin Xing, Yude Zhang*

J. Rare Earths, (38) 2020: 1003-1008

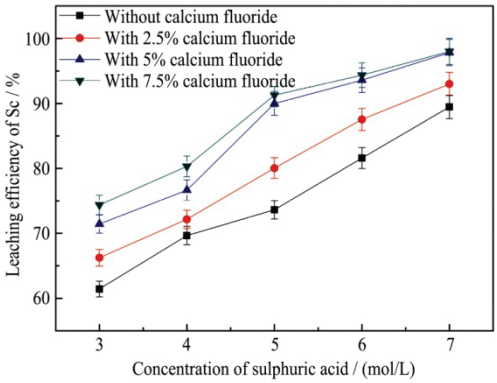

The CaF_2can obviously improve the leaching efficiency of Sc and reduce the acid consumption. The leaching efficiency of Sc is 70%, 78%, 90%, and 92%, respectively with 0, 2.5%, 5%, and 7.5% of CaF_2 at 5 mol/L H_2SO_4. Furthermore, the leaching efficiency of Sc also increases with an increase of H_2SO_4 concentration at the same amount of CaF_2

1009 Kinetics study on leaching of rare earth and aluminum from polishing powder waste using hydrochloric acid

Xitao Wu, Zhijian Wang, Chuping Xia, Xuefeng Shi, Tianzong Luo, Xinjun Bao, Rongli Liu, Shengzhong Xie***

J. Rare Earths, (38) 2020: 1009-1018

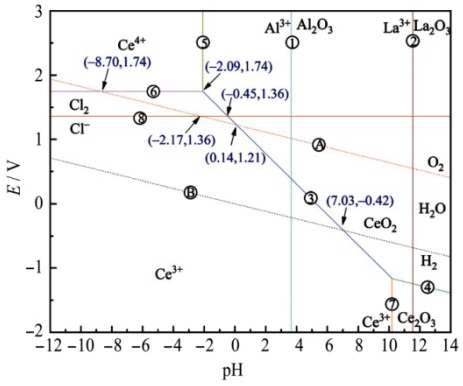

CeO_2 and HCl may react as follows: $4CeO_2 + 12HCl = 4CeCl_3 + O_2 + 6H_2O$

1019 Decomposition of mixed rare earth concentrate by NaOH roasting and kinetics of hydrochloric acid leaching process

Mei Li, Jianfei Li, Dongliang Zhang, Kai Gao, Huihui Wang, Wei Xu, Jinlong Geng, Xiaoyan Zhang, Xiufen Ma*

J. Rare Earths, (38) 2020: 1019-1029

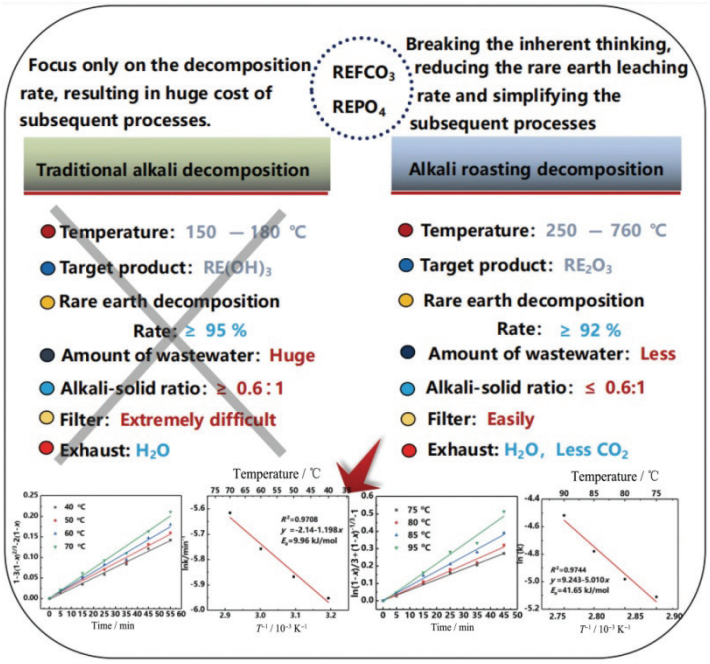

A smelting method for clean extraction of Bayan Obo mixed rare earth concentrate is reported. The reaction process is strengthened by optimizing the reaction mechanism, regulating the phase structure of the product, and increasing the reaction temperature. Therefore, it fundamentally overcomes a series of technical problems such as difficulty in traditional alkali decomposition and filtration, a large amount of water washing, and easy occurrence of "splashing" accidents. It has important practical significance and research value for the realization of the clean extraction of rare earth resources and associated elements of Bayan Obo

1030 Effect of titanium and rare earth microalloying on microsegregation, eutectic carbides of M2 high speed steel during ESR process

Fuxing Yin, Lu Wang, Zhixia Xiao[*], *Jianhang Feng, Lin Zhao*

J. Rare Earths, (38) 2020: 1030-1038

Alloy no.		Element segregation C	W	Cr	Mo	V
M2	C_d	0.10	3.60	3.36	2.84	1.51
	$k(=\frac{C_d}{C_i})$	**0.18**	**0.76**	**0.77**	**0.57**	**0.61**
M2RE	C_d	0.13	3.20	3.70	3.08	1.53
	$k(=\frac{C_d}{C_i})$	**0.62**	**1.01**	**0.87**	**0.95**	**1.03**
M2Ti	C_d	0.13	3.90	3.40	2.90	1.50
	$k(=\frac{C_d}{C_i})$	**0.80**	**1.01**	**0.93**	**0.95**	**0.97**
M2RETi	C_d	0.30	3.85	3.26	2.85	1.55
	$k(=\frac{C_d}{C_i})$	**0.55**	**0.88**	**0.78**	**0.70**	**0.76**

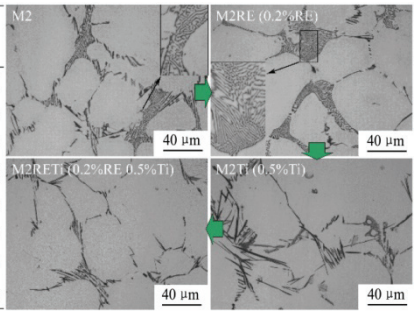

In-situ Ti microalloying during ESR significantly reduces dendritic segregation of M2 high speed steel, and changes the morphology of M_2C carbides from rod-like or maze-like to coarse feathery shape. *In-situ* Ti and RE composite microalloying improves the feather-like M_2C carbides, making them thinner and shorter, and tends to be isolated or distributed in a discontinuous network